


## Effect of the parameters affecting the properties during friction stir welding of AA 5083 H111 alloy

M. Merzoug <sup>1</sup> ✉, A. Ghazi<sup>2</sup>, A. Lousdad<sup>1</sup>, N. Benamara<sup>1</sup>,  
A. Miloudi<sup>1</sup>, A. Boulenouar<sup>1</sup>

<sup>1</sup>Laboratory of Materials and Reactives Systems, University of Djillali Liabes, Sidi Bel Abbes, Algeria

<sup>2</sup>Laboratory of Materials and Reactives Systems, University of Mustapha Stambouli, Mascara, Algeria

✉m\_merzoug01@yahoo.fr

**Abstract.** This research topic focuses on the friction stir welding (FSW) process. The study focuses on the correlation between the process parameters (feed speed and rotational speed) and the mechanical and microstructural characteristics of the 5083 H111 aluminum alloy sheets 4 mm thick placed end-to-end and welded by a vertical milling machine from. This experimental approach is based on the variation of the depth of penetration of the shoulder of the tool, allowing to contribute to mastering the axial force in order to predict the welding process area for this grade of aluminum by the welding process FSW. Then, tensile and hardness test were done to investigate the mechanical properties of the weld. The optimum process parameters were determined with reference to grain size, ultimate tensile strength and hardness. In addition, microhardness profiles allow to give the importance of the influence of the studied parameters on the different zones of the weld.

**Keywords:** FSW, aluminum alloys, penetration, pin and fracture surface

**Citation:** Merzoug M, Ghazi A, Lousdad A, Benamara N, Miloudi A, Boulenouar A. Effect of the parameters affecting the properties during friction stir welding of AA 5083 H111 alloy. *Materials Physics and Mechanics*. 2023;51(5): 116-125. DOI: 10.18149/MPM.5152023\_12.

### Introduction

Friction stir welding as a relatively new welding technique has gained wide applications in different industries such as aerospace, automotive and maritime [1–3]. This welding technique is essentially based on mechanical process in order to generate a temperature rise in the panels to be assembled. Producing the good quality welds is of great importance in many engineering applications. The maximum temperature created by the friction stir welding (FSW) process ranges from 70 to 80 % of the melting temperature of the welding material [4]. Low heat input during FSW prevents solidification failure and high temperature damage [5]. The development of a sound welds through FSW is more challengeable compared to the other welding techniques due to highly sensitivity to the welding parameters [6]. In a study, the highest tensile strength achieved was about 263 MPa and the defect-free joint was obtained by using the threaded tapered cylindrical pin tool at a rotational speed of 800 rpm [7]. In other study, analysis reveals that the nugget zone (NZ) exhibits recrystallized fine grains with an equiaxed structure as a result of dynamic recrystallization (DRX), resulting in improved mechanical properties of the joint [8,10]. Saravanakumar et al. [11,12] studied that the mechanical properties of the AA5083 UWFSW joint, such as its average ultimate tensile

strength and hardness, have been greatly improved using a straight hexagonal tool profile, tool rotational speed of 1200 rpm and welding speed of 20 and 40 mm/min.

In dissimilar joining of AA7075T651 retreating side and AA2024T351 advancing side investigated on the radius of pin flute with rotation speed 900 RPM, weld speed 150 mm/min of maximum tensile strength is 424 MPa with an efficiency of 94.3 % tool used threaded pin of flat cone for weld strength and joint strength truncated pin threaded tool is used and hardness of the weld is on soft metal of the heat affected zone [12,13]. Dissimilar joining of aluminum alloys by controlled temperature weld of tensile strength is improved on different clamping materials and backing of specially used for conjunction of weld speed 100 mm/min, rotational speed 900 rpm, tilt angle 30 and tensile strength is 426 MPa, elongation 7.1 % and efficiency of joint strength is 94.8 %. Mehta et al. and Sato et al. [14] studied of 5456-T321 aluminum alloy plates of the lower is 2.5 mm sheet annealed with tools used threaded conical pin, cylindrical conical threaded pin, stepped conical threaded pin, flared triflute pin are used on input parameters of rotational speed 600 rpm and 800 rpm, micro hardness, microstructure on nugget weld, heat affected zone, thermomechanical affected zone with fine grain size 5  $\mu\text{m}$  with free defect joints with growth of grain are investigated.

In this study, the hardness distribution and mechanical tensile properties of plates welded by FSW with different rotational speeds and welding speeds were investigated to study the effect of welding parameters on mechanical properties and fracture behavior of FSW for aluminum alloy 5083 H111. For all configurations of welding performed, a joint coefficient  $C_j$  is evaluated for the qualification of the good mechanical strength of welded joints.

### Experimental method

In this investigation, distinct aluminium 5083 H111 sheets were welded using for different parameters. The chemical composition of this aluminium is presented in Table 1 and the mechanical properties of the sheets are presented in Table 2.

**Table 1.** Chemical composition of 5083 H111 aluminum alloy (BM)

Al	Si	Fe	Cu	Mn	Mg	Cr	Zn	Ti
0.15	0.40	0.40	0.10	0.10	4.90	0.25	0.25	0.15

**Table 2.** Mechanical properties of 5083 H111 aluminum alloy

E, MPa	YS, MPa	UTS, MPa	A, %	K, J/cm <sup>2</sup>	HV
71008	155	236	16.5	45	88

A retrofitted milling machine was used for all the FSW experiments. To restrain the thermal expanding and thus bulking behaviour of plates, which could otherwise be encountered during normal FSW conditions, a bolted clamping system was used in all experiments.

Welds were made using a mixing tool, in a high-alloy steel (X210Cr12) with a tensile strength  $R_m = 870$  MPa, a threaded cylindrical pin (7 mm diameter and 3.60 mm in length) and shoulder (25 mm diameter).

The process parameters used in the tests are listed in Table 3. All used sets of welding parameters allowed us to obtain defect-free weld faces. The most visible difference in the joints' appearance was the amount of flash, which increased together with the tool rotation speed. It is impossible to state unequivocally that the welding velocity in the used range (16–400 mm/min) has any impact on the formation of flash. An example photo of the joints produced with the different used welding velocity is presented in Fig. 1. This example illustrates the overall tendency of flash formation. For all tested values of welding velocity the

greatest flashes were obtained in joints produced with a tool rotation speed of 1400 rpm, pointing to the excessive material flow [15,16].

**Table 3.** Process parameters

$\omega$ , rpm	710	1000	1000	1400	2000
V, mm/min	16	16	40	40	40
	25	25	80	80	80
	50	50	100	100	100
	80	80	200	200	200
	150	150	400	400	400



(a)



(b)



(c)



(d)



(e)



(f)

**Fig. 1.** Example of welded joints obtained with different welding velocity:

(a)  $\omega = 710$  rpm,  $V = 80$  mm/min; (b)  $\omega = 1000$  rpm,  $V = 80$  mm/min;

(c)  $\omega = 1000$  rpm,  $V = 150$  mm/min; (d)  $\omega = 1000$  rpm,  $V = 16$  mm/min;

(e)  $\omega = 710, 1000, 1400$  rpm,  $V = 25, 50, 100$  mm/min; (f)  $\omega = 1000$  rpm,  $V = 100$  mm/min

The cutting operation of samples on the welded plates is shown in the diagram presented in Fig. 2, where the geometric dimensions are expressed in mm according to the American society for testing and materials (ASTM E8M-04) standards [17].

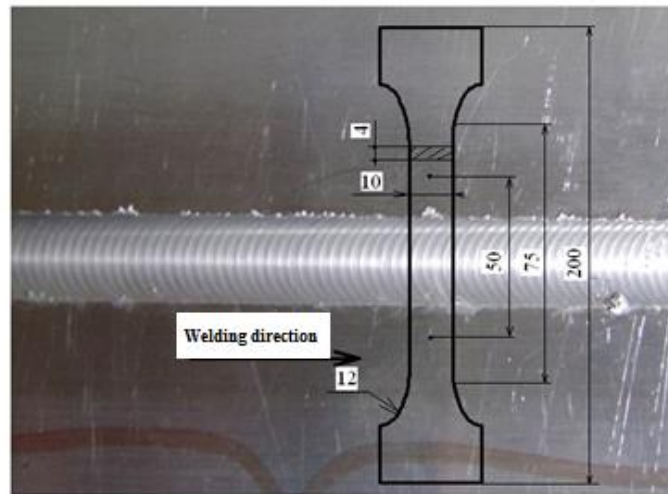


**Fig. 2.** Specimen preparation for tensile

Tensile tests were performed using a universal INSTRON tensile machine at a crosshead speed of 2 mm/min, controlled by the MTS software, as shown in Fig. 3. The broken tensile specimens after test is illustrated in (Fig. 3(b)). Profiles microhardness at mid-thickness of the joints; perpendicular to the axis of welding is performed. The measuring sockets are made every millimeter.



(a)











(b)

**Fig. 3.** Testing machine INSTRON: (a) tensile test specimen measured by the extensometer; (b) broken tensile specimens after test

## Results and Discussions

**Radiographic Inspection of Friction Stir Welds.** The results of the radiographic tests conducted on all the similar FSW weld joints produced at rotation speed of 710, 1000, 1400 rpm and transverse speed of 25, 50, 100 mm/min are hereby presented in Table 4. The defects found are mainly lack of penetrations, wormhole or voids. It can be seen from the results table that increasing the transverse speed increases the occurrence of defects. From the results, these weld flash is necessitated by material flow behavior, which is predominantly influenced by the FSW process parameters such as the tool rotational speed [18].

**Table 4.** Weld photographs and radiographs at different rotational and transverse speed

Weld photo	Radiograph	$\omega$ , rpm	V, mm/min	Observations
		710 rpm	25 mm/min	Lack of penetrations, hole left
		1000 rpm	50mm/min	Lack of penetrations, crack, incomplete fusion
		1400 rpm	100 mm/min	Lack of penetrations, wormhole defect, Sufficient mixing
		1000 rpm	150 mm/min	No evidence of root defects was observed on all the welds produced using the 700-rpm rotation speed and the feed rate 150 mm/min. Keyhole observed

**Microhardness profile and microstructure.** It is well-known that the hardness profile of the FSW joints with various welding parameters may be a direct indicator of microstructural and global mechanical properties evolution during FSW process [19]. Fig.4 shows the evolution of the hardness variations along the traverse weld section for various welding parameters. Generally, the typical profile of the microhardness of a welded joint FSW is a W shape. Indeed, this type of profile is characterized by two minimum values  $H_v$  of microhardness. These two points were located in the TMAZ. In the stirred zone (ZS), the microhardness value increases in comparison with the TMAZ, corresponding to the second minimum. It should be emphasized that the size of the ZS area is governed by the pin diameter, while the TMAZ area is generated by the size of the tool shoulder of the tool.

In addition, Fig. 1 shows that the TMAZ is the weakest region in a welded joint FSW. Whatever the welding parameters there has been a decrease in hardness in the HAZ which is due to the restoration phenomenon. This phenomenon is characterized by the recombination



and rearrangement of dislocations[20]. At the edge zones HAZ and TMAZ the granular structure is completely recrystallized. This recrystallization takes place near the TMAZ where a significant decrease in hardness is detected.

Figure 4 shows that a small welding speed value (40 mm/min, 1000 rpm) gives a small value of the microhardness equal to 33 HV in TMAZ region on both advancing side (AS) and retreating (RS). This 38 % degradation in hardness is mostly characterized in the TMAZ. This is attributed to a combination of high stresses and large strains resulting in the deformation of the grain structure, where re-crystallization did not take place, caused a coarse grain structure [18]. Thus, the roughly homogeneous hardness profiles could have an intimate relationship with the good thermal stability during FSW (Fig. 7). Finally, higher hardness values are attained at the welding speed of 200 mm/min as result of formation of a very fine grain structure. This result is not surprising because a small welding speed generates a high temperature in the seal, which creates a hot welding [21]. Therefore, it is clear that the failure of tensile specimens is often located in the TMAZ region or in a region between TMAZ and HAZ. On the other hand, the hardness values were reduced to a high welding speed because the temperature in the tool is reduced, thus leading to cold welding.

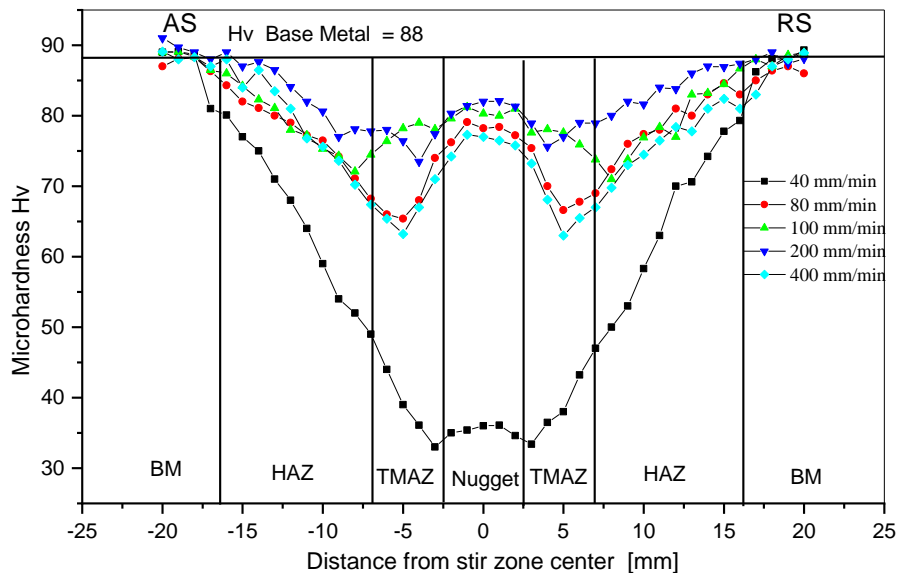


**Fig. 4.** Variation of the hardness for the rotational speed 1000 rpm

**Tensile strength.** The material was welded according to the above-mentioned specifications of different welding conditions. Tensile strength of the FSW joints was evaluated by conducting tests in a INSTRON 8516 universal testing machine. For each welded plate, specimens were prepared and tested. The fracture has occurred mostly in the HAZ on the retreating side of the weldment.

At low spindle speeds, frictional heat generation is less, which results in the poor plastic flow of material. Therefore, lower tensile strength was observed. At higher spindle speeds, frictional heat generation is high which enhances the plastic flow of material thus loses the tool material contact. So the poor stirring was obtained. At the highest welding speed of 200 mm/min and lowest welding speed of 80 mm/min, lower tensile strengths were observed.

Figure 5 shows the effects of welding parameters on the mechanical strength of welded joints, which are compared to the yield stress value of the base metal (155 MPa). We define the coefficient of joint efficiency as the ratio between the mechanical assembly and the mechanical properties of the base metal (Table 5). Where  $Y_s$  is the welded joint tensile elastic limit.

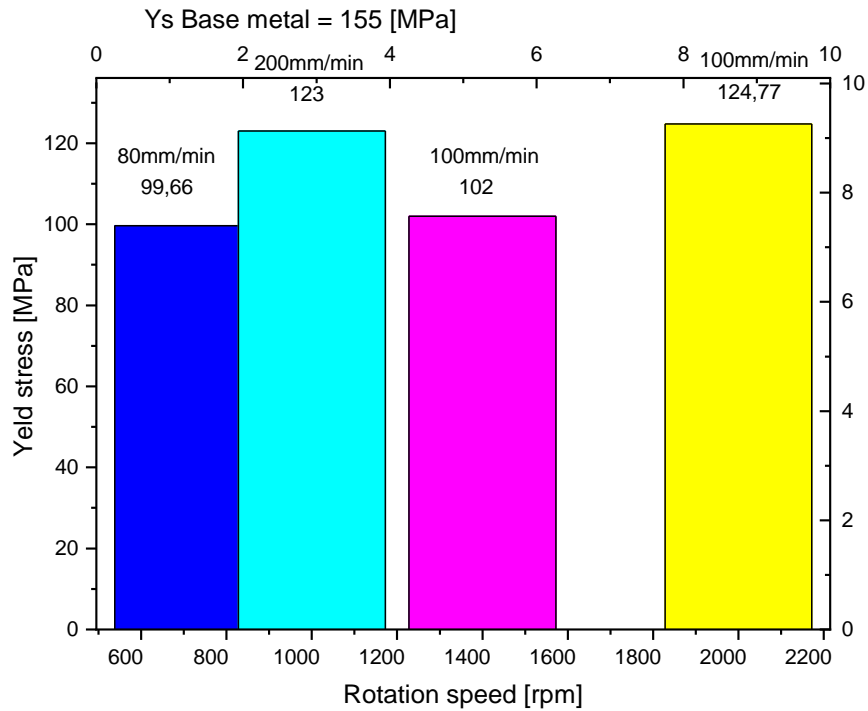


**Fig. 5.** Variation of the yield strength YS versus rotation speed and welding speed

**Table 5.** Tensile test results for welded specimens

N° of Sample	$\omega$ , rpm	V, mm/min	YS, MPa	UTS, MPa	Efficiency of joints, %	Fracture location
1	710	40	90	139.92	59.29	TMAZ
2	710	80	100	151.63	64.25	TMAZ
3	710	100	90	136.40	57.80	TMAZ
4	710	200	45	71.98	30.50	TMAZ
5	710	400	30	47.64	20.19	Nugget
6	1000	40	35	56.16	23.80	Nugget
7	1000	80	70	115.28	48.85	TMAZ
8	1000	100	110	173.55	73.54	TMAZ
9	1000	200	123	187.26	79.35	TMAZ
10	1000	400	60	95.29	40.38	TMAZ
11	1400	40	33	54.35	23.03	Nugget
12	1400	80	60	85.85	36.38	TMAZ
13	1400	100	105	155.28	65.80	TMAZ
14	1400	200	75	116.91	49.54	TMAZ
15	1400	400	55	83.28	35.29	TMAZ
16	2000	40	20	30.44	12.90	Nugget
17	2000	80	115	181.17	76.77	TMAZ
18	2000	100	123	189.95	80.49	TMAZ
19	2000	200	33	46.94	19.89	Nugget
20	2000	400	28	39.27	16.64	Nugget

This coefficient allows to estimate the reduction in strength due to the welding operation. For aluminum alloys, the coefficient for weld joint by FSW is of the order of 0.6 to 1 [22].

It was found that ultimate tensile strengths (UTS) of the joints were nearly equal a 50 % to those of the BM with the joint efficiency being 20–80%, and they were insensitive to changes in the welding parameter. However, the fracture behavior of the joints varied with the welding parameter. After the tensile test, FSWed specimens had fracture near TMAZ/HAZ at the retreating side. By applying the rolling process, it did not change the location of the fracture [23]. The fracture at the HAZ indicated that it was the weakest point of the welding area. This is because the grains in the HAZ experienced an annealing-like process by heat transfer from the NZ during welding. Hence, the grain size increased, whereas the mechanical properties and hardness decreased [24].

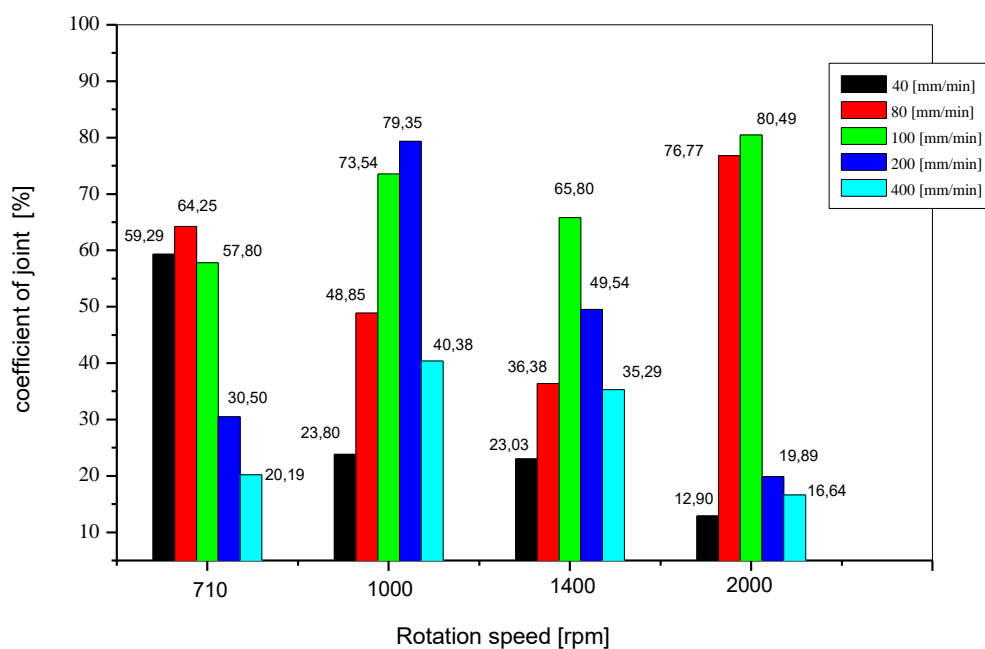


**Fig. 6.** Variation coefficient of joint versus welding speed for the rotational speed

The Figure 6 shows the variation of the coefficient of the joint for all welding parameters, such as rotational speed and the welding speed. From this figure, we see that the optimal values are obtained in the following ranges:

1. [710 rpm, 80 mm/min],
2. [1000 rpm, 100 mm/min], [1000 rpm, 200 mm/min],
3. [1400 rpm, 100 mm/min],
4. [710 rpm, 80 mm/min],
5. [1000 rpm, 100 mm/min], [1000 rpm, 200 mm/min],
6. [1400 rpm, 100 mm/min],

From these results, one can draw the optimum values for the rotational speed and the welding speeds. The results correspond to the welding speed 100 mm/min gives optimal results that there is a stability.

**Macroscopic fracture surface.** Fig. 7 shows the fracture surfaces for all configurations of FSW tested in this investigation. The dimple shape on the surface highlights the ductile behaviour of the samples [25]. It is noted that the most homogeneous facies located for the conditions for speed 1000 and 1400 rpm and the welding speed 40 to 200 mm/min. But the



choice of low welding speed leads to an increase in the welding time, therefore ideal for the industry to take welding speed between 100 and 200 mm/min. Therefore, FSW is considered an effective method, and it gives long life welds due to the modification of microstructure which leads to the improvement of mechanical properties [26]. In addition, the heat input reduction leading to reduction in the thickness of TMAZ and HAZ which and reduction in recrystallized grain size, in turn, increases the tensile strength of the joint [27].

The facies of rupture for the speed 2000 rpm present the following observations:

1. High heat generation and strong mixing in the shoulder;
2. The material is led under the shoulder at the root;
3. Appearance of two cores;
4. Appearance of a defect of the type “wormhole”.

The fracture of the facies for high welding speed 400 mm/min: the minimum boundary layer for steady motion of the material is not reached, lack of material at the root [20].

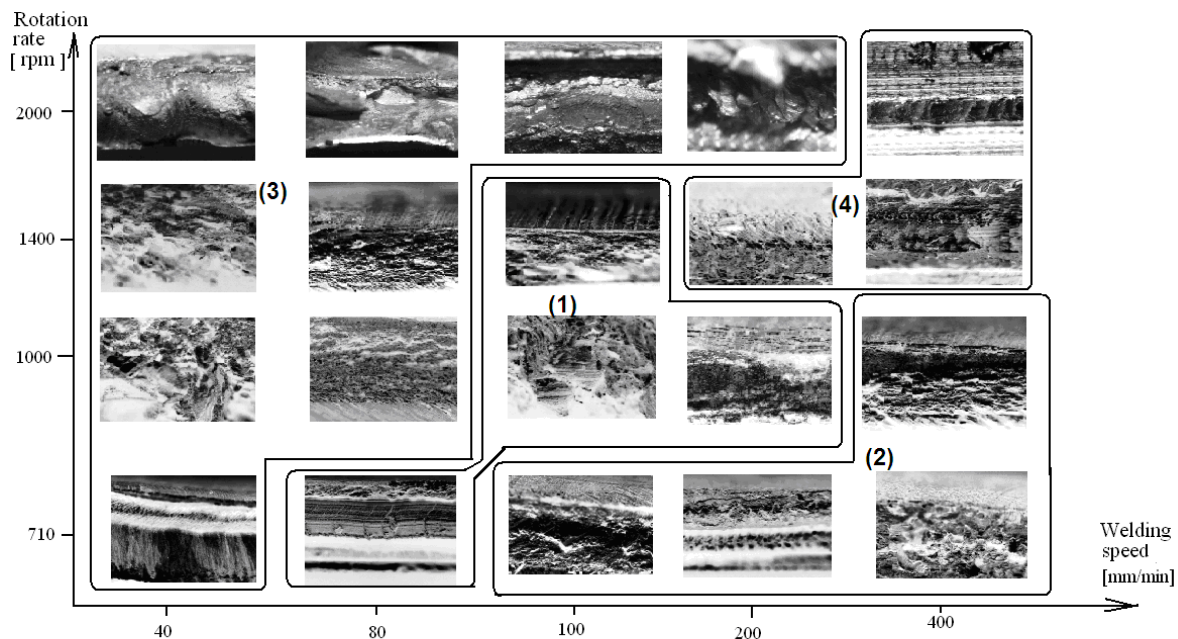


**Fig. 7.** Fracture surface of the alloy FSW 5083 H111

### Conclusions

In this experiment, it is observed that the process parameters like tool design, tool rotational speed, and welding speed are the main parameters to produce the butt joint by friction stir welding. It can be concluded that by varying the process parameters within the range:

1. The hardness distribution and mechanical tensile properties of plates welded by FSW with different rotational speeds and welding speeds were investigated to study the effect of welding parameters on mechanical properties and fracture behavior of FSW for aluminum alloy 5083H111;
2. Ultimate tensile strengths (UTS) of the joints were nearly equal a 50% to those of the BM, with the joint efficiency being 20–80 %;
3. Tensile strength increases with increase of tool rotational speed;
4. Tensile strength of base material is 155 MPa; it means the joint efficiency is 76 to 80 %;
5. The microstructure of the weld zone be dominated by recrystallization caused by the thermal excursion of the unstable base material, resulting in a wide zone of equiaxed grains around the weld line. Increasing the traverse narrows this weld zone.

## References

1. Akbari M, Abdi Behnagh R. Dissimilar friction-stir lap joining of 5083 aluminum alloy to CuZn34 brass. *Metallurgical and Materials Transactions B*. 2012;43(11): 77–86.
2. Behnagh RA, Besharati Givi MK, Akbari M. Mechanical properties, corrosion resistance, and microstructural changes during friction stir processing of 5083 aluminum rolled plates. *Materials and Manufacturing Processes*. 2011;27: 636–640.
3. Shojaeefard MH, Behnagh RA, Akbari M, Givi MKB, Farhani F. Modelling and Pareto optimization of mechanical properties of friction stir welded AA7075/AA5083 butt joints using neural network and particle swarm algorithm. *Materials and Design*. 2013;44:190–198.
4. Campanelli S L, Casalino G, Casavola C, Moramarco V. Analysis and Comparison of Friction Stir Welding and Laser Assisted Friction Stir Welding of Aluminum Alloy. *Materials*. 2013;6: 5923–5941.
5. Saravana R, Linsha P, Harshini N, Rajasekaran T. Numerical Modelling of Thermal Phenomenon in Friction Stir Welding of Aluminum Plates AA5083 Military Grade Aluminium Alloy Joints in Underwater. *AIP Conference Proceedings*. 2022;2460: 070006.
6. Saravanakumar R, Rajasekaran T, Pandey C, Menaka M. Mechanical and Microstructural Characteristics of Underwater Friction Stir Welded AA5083 Armor-Grade Aluminum Alloy Joints. *Journal of Materials Engineering and Performance*. 2022;31: 8454–8472.
7. Azmi MH, Hasnol MZ, Zaharuddin MFA, Sharif S, Rhee S. Effect of tool pin profile on friction stir welding of dissimilar materials AA5083 and AA7075 aluminium alloy. *Archives of Metallurgy and Materials*. 2022;67(2): 465–470.
8. Saravanakumar R, Rajasekaran T, Pandey C, Menaka M. Influence of Tool Probe Profiles on the Microstructure and Mechanical Properties of Underwater Friction Stir Welded AA5083 Material. *Journal of Materials Engineering and Performance*. 2022;31: 8433–8450.
9. Patil C, Patil H, Patil H. Investigation on Weld Defects in Similar and Dissimilar Friction Stir Welded joints of Aluminium Alloys of AA7075 and AA6061 by X-ray Radiography. *American Journal of Material Engineering and Technology*. 2016;4(1): 11–15.
10. Saravanakumar R, Rajasekaran T, Pandey C. Optimisation of underwater friction stir welding parameters of aluminum alloy AA5083 using RSM and GRA. To be published in *Proceedings of the Institution of Mechanical Engineers, Part E: Journal of Process Mechanical Engineering*. [Preprint] 2023. Available from: doi.org/10.1177/09544089231158948.
11. Saravanakumar R, Rajasekaran T, Pandey C. Underwater Friction Stir Welded Armour Grade AA5083 Aluminum Alloys: Experimental Ballistic Performance and Corrosion Investigation. To be published in *Journal of Materials Engineering and Performance*. [Preprint] 2023. Available from: doi.org/10.1007/s11665-023-07836-2.
12. Salari E, Jahazi M, Khodabandeh A, Nanesa HG. Friction stir lap welding of 5456 aluminium alloy with different sheet thickness: process optimization and microstructure evolution. *International Journal of Advanced Manufacturing Technology*. 2016;82; 39–48.
13. Girish G. Effect of tool pin geometry and multi-pass intermittent friction stir processing on the surface properties of aerospace grade aluminium 7075 alloy. To be published in *Journal of Process Mechanical Engineering*. [Preprint] 2023. Available from: doi.org/10.1177/09544089231158948.
14. Mehta P K, Badheka J V. Influence of tool design and process parameters on dissimilar friction stir welding of copper to AA6061-T651 joints. *International Journal of Advanced Manufacturing Technology*. 2015;80; 2073–2082.
15. Kosturek R, Sniezek L, Torzewski J, Wachowski M. The Influence of Welding Parameters on Macrostructure and Mechanical Properties of Sc-Modified AA2519-T62 FSW Joints. *Manufacturing Review*. 2020;7:28.

16. Kosturek R, Torzewski J, Wachowski M, Sniezek L. Effect of Welding Parameters on Mechanical Properties and Microstructure of Friction Stir Welded AA7075-T651 Aluminum Alloy Butt Joints. *Materials*. 2022;15: 5950.
17. Chekalil I, Miloudi A, Planche MP, Ghazi A. Prediction of mechanical behavior of friction stir welded joints of AA3003 aluminum alloy. *Frattura ed Integrità Strutturale*. 2020;14(54): 153–168.
18. Mumvenge I, Akinlabi Stephen A, Mashinini PM, Fatoba S, Okeniyi J, Esther T, Akinlabi ET. Evaluation of Friction Stir Welds by X-ray Digital Radiographic Non- Destructive Approach. *Materials Science and Engineering*. 2018;413:012035.
19. Cavaliere P, Squillace A, Panella F. Effect of welding parameters on mechanical and microstructural properties of AA6082 joints produced by friction stir welding. *Journal of Materials Processing Technology*. 2008;200(1-3): 364–372.
20. Edwards P, Ramulu M. Peak temperatures during friction stir welding of Ti–6Al–4V. *Science and Technology of Welding and Joining*. 2010;15(6): 468–472.
21. Ahmed MMZ, Ataya S, El-Sayed Seleman M M. Heat input and mechanical properties investigation of friction stir welded AA5083/AA5754 and AA5083/AA7020. *Metals*. 2021;11(1): 68.
22. Moraitis GA, Labeas GN. Investigation of friction stir welding process with emphasis on calculation of heat generated due to material stirring. *Science and Technology of Welding and Joining*. 2010;15(2):177–184.
23. Tao Y, Zhang Z, Ni D R, Wang D, Xiao B L, Ma Z Y. Influence of welding parameter on mechanical properties and fracture behavior of friction stir welded Al–Mg–Sc joints. *Materials Science & Engineering A*. 2014;612: 236–245.
24. Selamat N M, Baghdadi A H, Sajuria Z. Effect of Rolling on Strength of Friction Stir Welded Joint of Aluminium Alloys. *Jurnal Kejuruteraan SI*. 2018;1(6): 9–15.
25. Abdul LN, Sajuri Z, Syarif J. Effect of aluminium content on the tensile properties of Mg–Al–Zn alloys. *Jurnal Kejuruteraan*. 2014;26: 35–39.
26. Marhoon II, Al-Kamal AK, Abdulrehman MA. Studying the Mechanical Properties for 5086 Aluminum Alloy Welded Plates by Friction Stir Welding (FSW). *International Conference On Materials Engineering and Science*. 2018;454: 012084.
27. Chandan P. Mechanical and Metallurgical Characterization of Dissimilar P92/SS304 L Welded Joints Under Varying Heat Treatment Regimes. *Metallurgical and Materials Transactions A*. 2020;51: 2126–2142.

## THE AUTHORS

**M. Merzoug** 

e-mail: m\_merzoug01@yahoo.fr

**A. Lousdad**

e-mail: a\_lousdad@yahoo.com

**A. Miloudi**

e-mail: miloudidz@yahoo.fr

**A. Ghazi**

e-mail: ghaziaek@yahoo.fr

**N. Benamara**

e-mail: benamara96@yahoo.fr

**A. Boulenouar**

e-mail: aek\_boulenouar@yahoo.fr